

Electronic Supplementary Information for

Dynamic interplay between interfacial nanobubbles: Oversaturation promotes anisotropic depinning and bubble coalescence

Sarthak Nag,^{†ab} Yoko Tomo,^{†a} Hideaki Teshima,^{bc}

Koji Takahashi,^{bc} Masamichi Kohno^{*ab}

^a Department of Mechanical Engineering, Kyushu University, Fukuoka 819-0395, Japan

^b International Institute for Carbon-Neutral Energy Research (WPI-I2CNER), Kyushu University, Fukuoka 819-0395, Japan

^c Department of Aeronautics and Astronautics, Kyushu University, Fukuoka 819-0395, Japan

*Corresponding Author: kohno@mech.kyushu-u.ac.jp

†Equal Authorship

Supplementary Information 1

Movie M1 is included as supplementary material for this manuscript.

Legend for Movie M1: TEM movie of the anisotropic depinning and pull-push phenomenon observed in the surface nanobubbles.

Supplementary Information 2

(Additional Figures and Plots)

Static contact angle of water on the SiN_x window

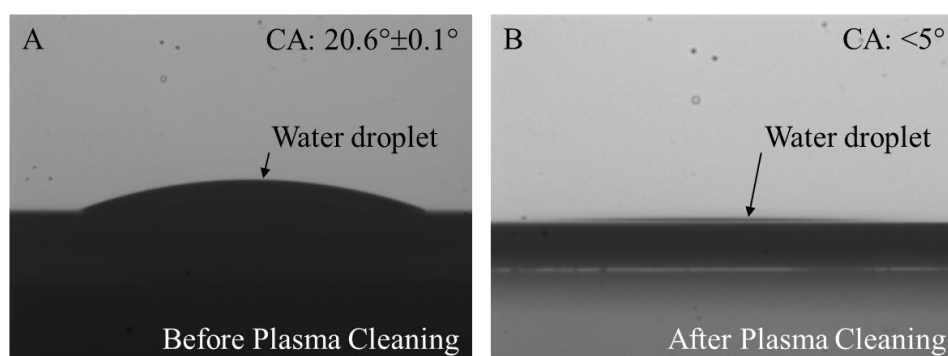


Figure S1. Static contact angle of the water droplet on the SiN_x window, before and after the plasma treatment. The plasma treatment rendered high hydrophobicity to the surface, thus making the contact angle $<5^{\circ}$. The contact angles were measured using the half-angle method ($\theta = 2 \tan^{-1}(h/r)$).

◆ Time history of observed nanobubbles

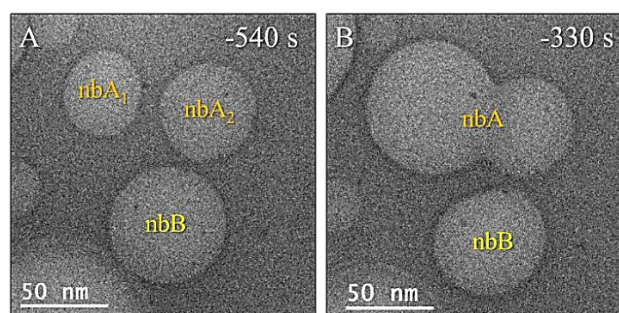


Figure S2. Time history of the nanobubbles A and B. **A.** Nanobubble *nbA* was formed after the coalescence of *nbA*₁ and *nbA*₂. **B.** *nbA* during the merging process of its two constituent nanobubbles. The shape formed by *nbA* during merging reverifies that the formed bubble is a surface nanobubble. *nbB* is a pinned surface nanobubble, exhibiting deformation induced due to its neighboring nanobubbles. Scale bar: 50 nm.

◆ Interactions between the nanobubbles present on adjacent SiN_x window

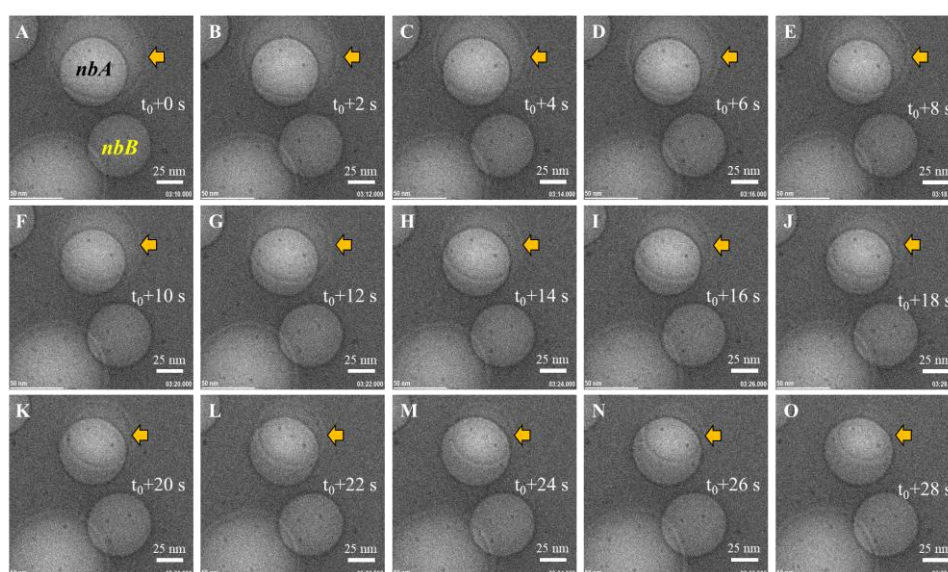


Figure S3. Time sequence TEM images of the nanobubbles *nbA*, *nbB* and the other nanobubbles (discussed in the manuscript) observed on the adjacent SiN_x window. Yellow arrow shows the contact line of the nanobubble present on the top window. As this nanobubble shrinks, no changes were observed in the shape and size of *nbA*. This demonstrates that the behavior of the top bubble does not induce any remarkable size changes in *nbA* persistently, and the interactions between *nbA* and *nbB* are stronger due to lower interfacial distance between them. Scale bar: 25 nm.

◆ Nanobubble contact area and interfacial gap before the observed phenomenon

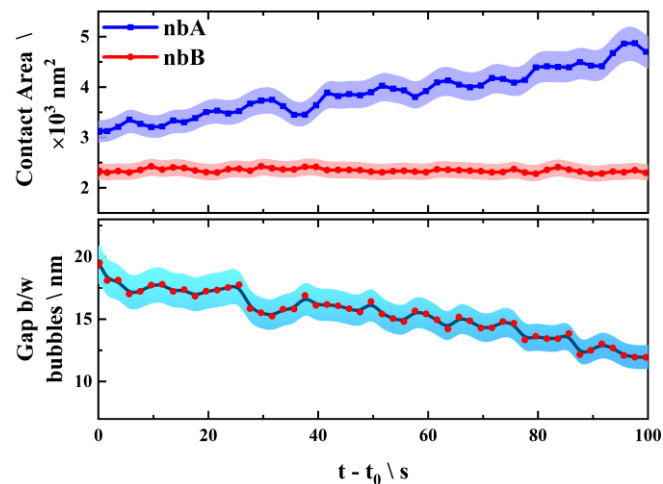


Figure S4. Variation of nanobubble contact area and the gap between their 3-phase contact lines before the observed phenomenon. **A.** The *nbA* is a growing nanobubble, exhibits a growth rate of $\sim 17 \text{ nm}^2/\text{s}$ for the initial 100 s. The *nbB* is a strongly pinned nanobubble and exhibits negligible changes in its contact area. **B.** The gap between their 3-phase contact lines reduces monotonically from 20 nm to 12.5 nm in 100 s.

◆ Time sequence TEM images of the pull-push phenomenon and anisotropic depinning observed in other nanobubbles

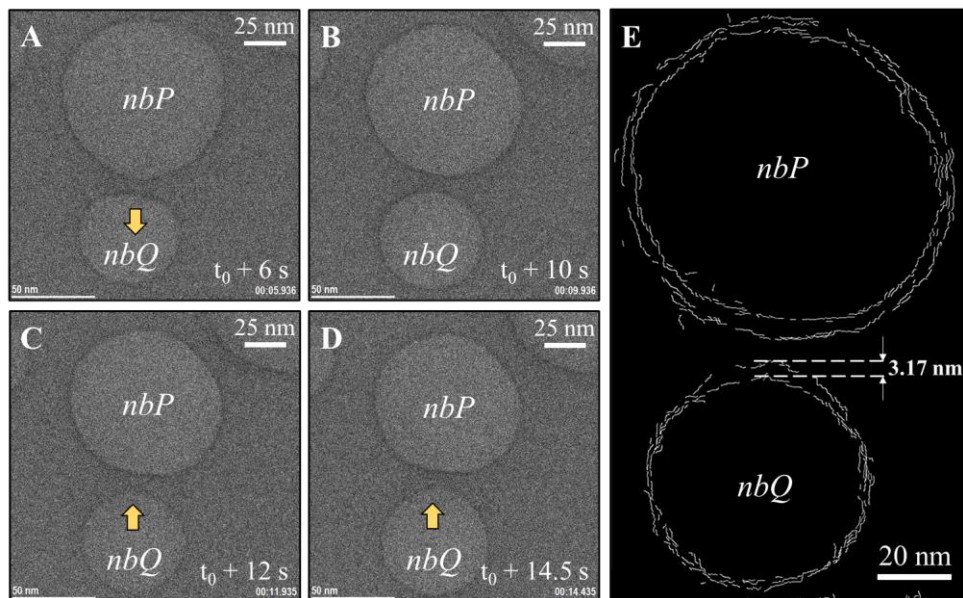


Figure S5. (A-D) Time sequence TEM images of the observed pull-push phenomenon observed in another nanobubble pair (*nbP* and *nbQ*). The yellow arrow shows the direction of the contact line's movement and distortion in nanobubble induced due to the growth and shrinking of the other nanobubble. The magnitude of the depinning in the bubble was observed to be less as compared to

the results discussed in the manuscript, possibly due to the lower oversaturation. In the presented images, the electron beam intensity measured was $\sim 0.32 \text{ A/cm}^2$, while for the images presented in the main manuscript, the electron beam intensity was $\sim 1.03 \text{ A/cm}^2$. Scale bar: 25 nm. **(E)** Edge detected overlapped image of the nanobubbles observed at $t=t_0+10 \text{ s}$ and $t = t_0+14.5 \text{ s}$. The extend of depinning is highlighted in the image. Scale bar: 20 nm.

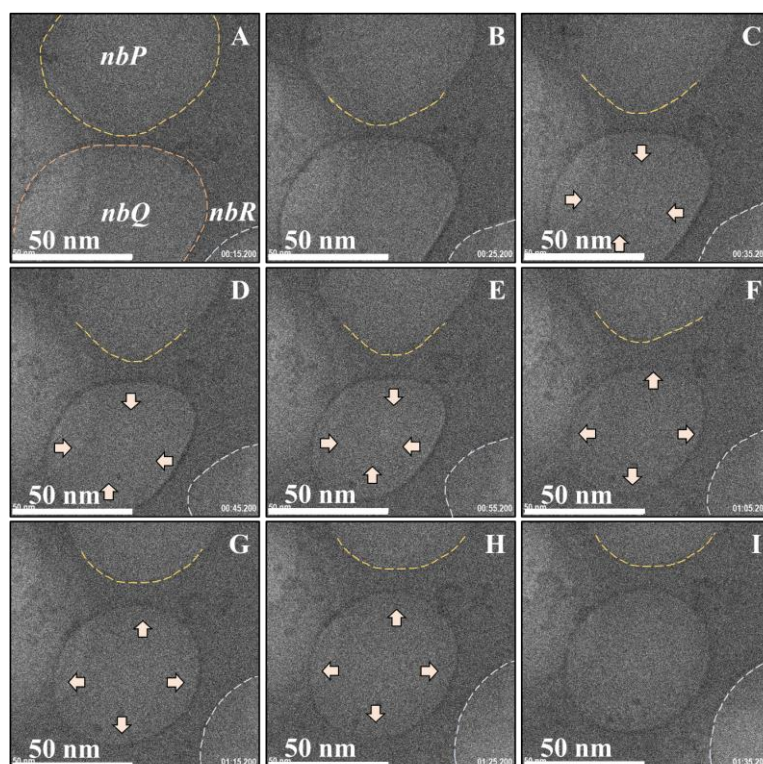


Figure S6. (A-I) Time sequence TEM images of three nanobubbles demonstrating anisotropic depinning. The time interval between each image frame is 10 s. The initial positions of the 3-phase contact lines of nanobubbles *P*, *Q* and *R* are shown in **(A)**. Nanobubble *Q* begins shrinking, which leads to the distortion in the adjacent interfaces of nanobubble *P* and *R*, as shown in **(C)**, **(D)** and **(E)**. After $\sim 50 \text{ s}$, nanobubble *Q* exhibits growth, as shown in **(F-H)**, which increases the circularity of the 3-phase contact line of nanobubble *P* and *R*. Scale bar: 50 nm.

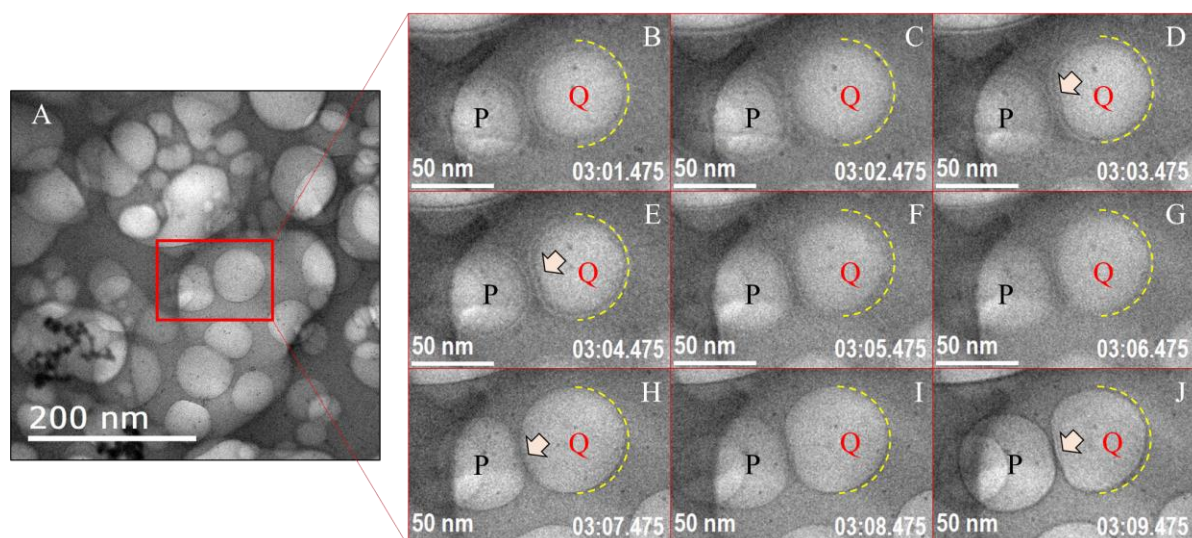


Figure S7. (A) TEM image of multiple nanobubbles nucleated in a single image frame. Scale Bar: 200 nm. (B-J) Time sequence TEM images of two nanobubbles (*P* and *Q*) exhibiting pull-push phenomenon. Images (B-G) are captured while the bubbles are over-focus (bright fringes around the bubble), whereas images (H-J) are captured while the bubbles are under-focus (dark fringes). The yellow dotted curve highlights the pinned three-phase contact line of nanobubble *Q*. Due to the size fluctuations of *P*, distortion in the three-phase contact line of nanobubble *Q* close to the nanobubble *P* is observed, which has been highlighted by an arrow in (D, E, H and J). Scale bar: 50 nm.

◆ **Long term variation of the mean radii of nanobubbles nbA and nbB**

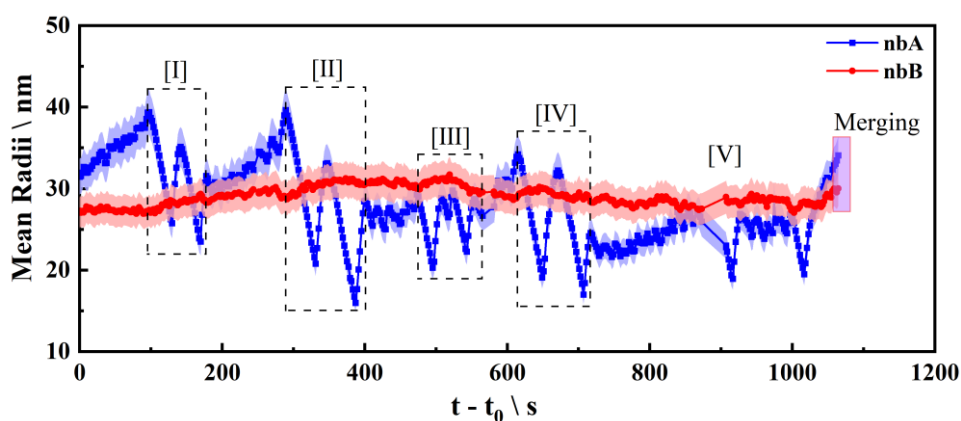


Figure S8. Variation of mean radii ($\sqrt{\text{area}/\pi}$) of nanobubbles *nbA* and *nbB* during the complete observation of ~ 18 minutes. *nbA* exhibits high variations in its radius and is deemed as unpinned nanobubble. *nbB* has low variations due to the strong pinning of its contact line. Series of shrink-growth behavior of *nbA* were observed in the study, as depicted by dotted rectangles [I] – [V]. The merging of nanobubbles was observed at 1065 s.